

# Non-linear propagation of limited diffraction beams

Johan-Fredrik Synnevåg and Sverre Holm  
Department of Informatics, University of Oslo  
P.O. Box 1080, N-0316 Oslo, Norway

*Abstract*—Recently, harmonic imaging has been shown to increase image quality in medical imaging. This is believed to be caused by decreased sidelobes. It is also due to a decreased sensitivity to near-field aberrations owing to the lower transmission frequency, and the lower relative amplitude of the second harmonic in the near-field.

One of the problems of limited diffraction beams has been the sidelobe level. We performed a simulation of non-linear propagation for Bessel beams and X waves to see what performance gains that could be achieved. We used the angular spectrum method of Christopher and Parker which includes a non-linear substep to predict higher harmonic generation. Simulations of continuous wave Bessel beam excitation on a 15 mm transducer at 2.275 MHz showed about 9 dB decrease in sidelobe level for the second harmonic. The beamwidth was approximately the same as for the first harmonic. Near the end of the depth of field, the sidelobes increased and gave a poorer beamprofile. For pulsed X wave excitation on the same transducer, high sidelobes were present throughout the depth of field. A large 50 mm Bessel transducer at 1.65 MHz gave a second harmonic with half the beamwidth and the same sidelobe level as the first harmonic.

By deleting the central lobe of the  $J_0$  Bessel beam for the 15 mm transducer, improved second harmonic properties were achieved. The second harmonic beam was characterized by low amplitude in the near-field, a narrow beam and reduced sidelobe level even for large depths. However, the modified Bessel beam loses some of its limited diffraction properties. Comparable results were achieved for the modified X wave, where the second harmonic also showed less energy in the X branches. The modified Bessel beam was compared to a spherically focused beam and showed about the same second harmonic beamwidth at the focal point, and 6 dB sidelobe reduction compared to the first harmonic of a conventional Bessel beam. Outside the focal area, the width of the spherically focused beam increased, while the modified Bessel beam remained narrow for a large depth of field.

## I. INTRODUCTION

Medical ultrasound transducers usually transmit a spherically focused beam, resulting in an optimal focal area, where the beam is narrow and the sidelobes are low. However, when moving away from the focal area, the beam gets broader, giving reduced contrast and resolution. Non-diffracting solutions to the linear wave equation have been found which overcome the problem of decreased resolution outside the focal plane. The theoretical non-diffracting beams have equal focus for all depths traveling to infinity, which means that the lateral field distribution is the same in every plane normal to the direction of propagation. One non-diffracting solution to the wave equation was studied by Durnin [1] and has been termed the Bessel beam. This beam is a plane wave shaded by a  $J_0$  Bessel-function, thereby the name. Lu and Greenleaf [2] has later given a solution in the form of X waves, which are non-diffracting pulses with similar focal properties as the Bessel beam. While the theoretical beams are non-diffracting for infinite distance, they require infinite aperture, and also infinite bandwidth for the X waves, to be exactly realized. Finite aperture realizations have only an approximately depth-independent shape for a finite distance and have been termed limited diffraction beams.

This work was partly sponsored by the ESPRIT program of the European Union under contract EP 22982

The problem with limited diffraction beams is high sidelobes. The lateral distribution of the zeroth-order Bessel beam is the  $J_0$  Bessel-function giving a sidelobe level of about  $-8$  dB. Effort has been made to reduce the sidelobes with various techniques [3], usually based on several transmissions and addition or subtraction of results. Our approach was to see if performance gain could be achieved based on non-linearity in the medium which the beams propagate through. Harmonic imaging, which takes advantage of non-linear distortion of sound beams as they propagate, has been shown to give improved image quality due to decreased sidelobes and a narrower second harmonic mainlobe. Applied to transmission of limited diffraction beams, the high sidelobe level was expected to decrease, while still maintaining good focal properties for a large depth of field.

## II. LIMITED DIFFRACTION BEAMS

The  $J_0$  Bessel beam is given by [1]

$$P_{B_0} = J_0(\alpha r) e^{j(\eta z - \omega t)} \quad (1)$$

where  $J_0$  is the zeroth-order Bessel-function,  $r$  is radius and  $\alpha$  and  $\eta$  are related to wavenumber,  $k$ , by

$$\alpha^2 + \eta^2 = k^2 \quad (2)$$

(1) represents an axially symmetric beam which is composed of plane waves traveling at angle  $\phi$  with respect to a plane normal to the z-axis, where  $\phi$  is given by

$$\phi = \sin^{-1}(\alpha/k) \quad (3)$$

The lateral beamwidth of the Bessel beam is given by the width of mainlobe of the Bessel-function in (1). The width of the mainlobe at half the peak value is given by

$$\text{FWHM}_{B_0} \approx 3.04/\alpha \quad (4)$$

Equation (1) represents single frequency waves, but broadband pulses are required for pulse-echo imaging. As (1) is simply a plane wave shaded by a Bessel-function, broadband Bessel beams could be generated by transmitting a broadband plane wave shaded by  $J_0(\alpha r)$ . This would however give a dispersive wave, since each frequency then travels at different angles as seen by (3). The X wave is a non-dispersive, non-diffracting solution to the wave-equation, given by [2]

$$P_{X_0} = \int_0^\infty B(k) J_0(kr \sin \phi) e^{-a_0 k + j(kz \cos \phi - \omega t)} dk \quad (5)$$

which is an integration over an infinite number of Bessel beams with  $\alpha$  adjusted so that each frequency component travels at the same angle ( $\alpha = k \sin \phi$  and  $\eta = k \cos \phi$ , given by (2) and (3)).

The  $e^{-a_0 k}$  factor makes the higher frequencies less significant, depending on  $a_0$ , making it possible to realize good finite bandwidth approximations.  $B(k)$  can be chosen to approximate the bandwidth of a transducer. The  $-6$  dB lateral beamwidth of the X wave is given by [2]

$$\text{FWHM}_{X_0} = 2\sqrt{3}/\sin\phi \quad (6)$$

Depth of field of both the Bessel beam and X wave is dependent on the angle  $\phi$  and size of the transducer, and is given by

$$\text{DOF} = R/\tan\phi \quad (7)$$

where  $R$  is the radius of the transducer. We see there is a tradeoff between large depth of field and a narrow beam, where a smaller  $\alpha$  (or smaller  $\phi$ ) gives larger depth of field, but a broader beam.

### III. NON-LINEAR WAVE PROPAGATION

In many applications sound propagation is assumed to be linear, which is not always a valid assumption. Recently, ultrasound imaging systems have taken advantage of soundbeam distortion due to the non-linear properties of tissue, giving images with improved quality. This is referred to as harmonic imaging. As the beam propagates, energy is transferred from the fundamental to higher harmonics, and reception is done at the second harmonic, or twice the transmitted frequency. The second harmonic of a focused beam is characterized by a narrower mainlobe and lower sidelobes compared to the first, giving better contrast and resolution. The lower transmit frequency also gives deeper penetration and less sensitivity to phase aberrations. Less sensitivity to near-field aberrations is also due to the lower relative near-field amplitude as second harmonic energy is generated as the beam propagates.

To simulate non-linear wave propagation we have used the angular spectrum method of Christopher and Parker [4], which is a quasi-linear method that solves the Burgers equation in the frequency domain by propagating a number of harmonics stepwise along the  $z$ -axis. The algorithm involves two substeps for propagating the field one step in the axial direction, a linear substep that accounts for diffraction and a non-linear substep that accounts for generation of higher harmonics.

As non-linear distortion is dependent on the initial pressure of the transducer, high source pressure is desirable to produce sufficient second harmonic energy to form an image. This may have undesirable bioeffects, something which is quantified by the Mechanical Index (MI), given by [5]

$$\text{MI} = \frac{p^-}{\sqrt{f_0}} \quad (8)$$

where  $p^-$  denotes maximum negative pressure in MPa, and  $f_0$  is the center frequency in MHz. The pressure amplitude should be found by calculating the maximum negative pressure in a medium with 0.3 dB/MHz/cm attenuation, and the center frequency should be estimated from the signal. In our simulations we have used the center frequency of the first harmonic for  $f_0$ , and  $p^-$  as the maximum pressure with the attenuation used in the simulations (0 or 0.3 dB/cm/MHz). All results are for an MI estimated in this way to be less than the safety limit of 1.9.

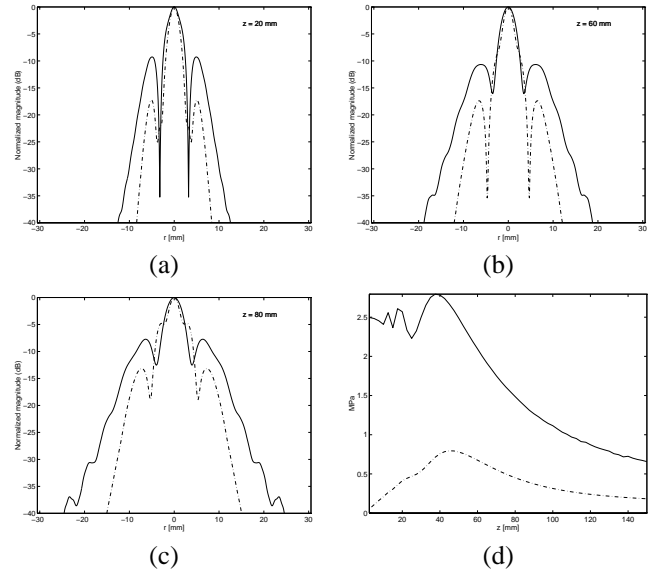


Fig. 1. First (solid line) and second (dotted line) harmonic of Bessel beam with  $\alpha = 736 \text{ m}^{-1}$ . (a), (b) and (c) Normalized lateral field distribution (dB) at  $z = 20, 60$  and  $80$  mm respectively (d) axial amplitude from  $z = 1 - 150$  mm, y-axis is pressure (MPa).

### IV. NON-LINEAR PROPAGATION OF LIMITED DIFFRACTION BEAMS

#### A. Bessel beam and X wave

Experiments have shown that the second harmonic of an unfocused piston and spherically focused transducer has both a narrower mainlobe and lower sidelobes compared to the first harmonic [6]. Applying nonlinear propagation conditions to the Bessel beam and X wave, the high sidelobe level was expected to decrease, while maintaining an approximately depth-independent focus for a large depth of field. We have simulated limited diffraction beam transmission from a 15 mm transducer with exact aperture shading, transmitting at 65% of the central frequency of 3.5 MHz [7].

Figure 1 shows simulations of the first and second harmonic of continuous wave Bessel beam excitation on the described transducer at various depths. Simulations were done in conditions similar to water with non-linearity parameter  $\beta = 3.5$ , and without attenuation. The aperture shading was chosen to include one sidelobe of the  $J_0$  Bessel-function, giving  $\alpha = 736 \text{ m}^{-1}$ . This gives a depth of field of 95 mm. Figures 1 (a) and (b) show about 9 dB decrease in sidelobe level of the second harmonic compared to the first, and about equal beamwidth. However, near the end of the depth of field, the sidelobes have grown, giving a poor beamprofile.

Figure 2 shows corresponding simulations of a broadband X wave focused in the same area. The X wave is generated by transmitting in a band centered at  $0.65 f_c$  (with  $-6$  dB bandwidth of about 1.77 MHz), and the second harmonic is found by calculating the pulse at the corresponding band at  $1.3 f_c$ , where  $f_c$  is the central frequency of the transducer. The lateral plots show that the second harmonic mainlobe is narrower, but high sidelobes are present throughout the depth of field. The high second harmonic sidelobes near the end of depth of field for the Bessel beam, which are present throughout the field for the X wave,

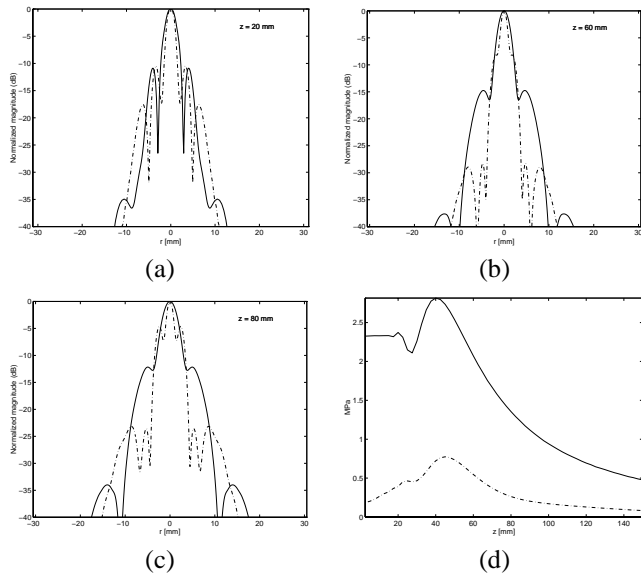


Fig. 2. First (solid line) and second (dotted line) harmonic of an X wave with  $a_0 = 0.05$  mm and  $\phi = 4.54^\circ$ . (a), (b) and (c) Normalized lateral field distribution (dB) at  $z = 20, 60$  and  $80$  mm respectively (d) axial amplitude from  $z = 1 - 150$  mm, y-axis is pressure (MPa).

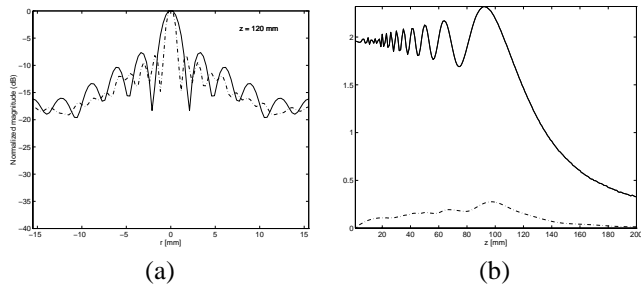


Fig. 3. First and second harmonic of Bessel beam produced by a 50 mm transducer with exact aperture shading and  $\alpha = 1202.45$ . Solid line represents the first harmonic, and dotted line represents the second harmonic (a) lateral field at  $z = 120$  mm (b) axial amplitude

seem to be so-called fingers or extra sidelobes and are probably caused by diffraction of the second harmonic as the beams propagate. The high extra sidelobes would then be expected to decrease if the beams were produced by a larger transducer. Figure 3 shows simulations of continuous wave Bessel beam excitation on the 50 mm Bessel transducer of [8] with exact aperture shading, transmitting at 65% of the central frequency of 2.5 MHz. The lateral plot in (a) is near the end of the depth of field. The second harmonic mainlobe is about half the width of that of the first harmonic and the extremely high sidelobes are no longer present, but there is little decrease in sidelobe level compared to the first harmonic.

This result resembles that predicted theoretically by [9] for an infinite aperture. They show that by inserting (1) in the Khoklov-Zabolotskaya-Kuznetsov (KZK) equation, the second harmonic beam is also a Bessel beam with twice the value for  $\alpha$ . This implies that the sidelobes are unchanged and that the mainlobe is half the width of that of the first harmonic. Our simulation in Fig. 3 is the one with the largest aperture and the one which is also closest to that result.

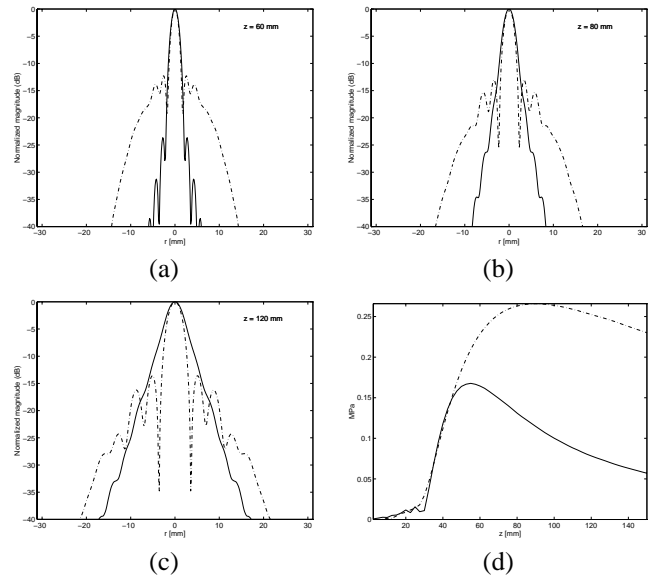


Fig. 4. Comparison of the second harmonic of a spherically focused (solid line) and modified Bessel beam (dotted line) (a), (b) and (c) lateral field (dB) at  $z = 60, 80$  and  $120$  mm (d) axial amplitude from  $z = 1 - 150$  mm.

### B. Modified Bessel beam and X wave

Assuming the high second harmonic sidelobes are caused by diffraction of the second harmonic as the beams propagate, generation of second harmonic energy further away from the transducer surface is desirable. This means that the first harmonic must be low near the transducer, which can be accomplished by deleting the central lobe of the Bessel-function in (1) and (5). Figure 4 shows a comparison of the second harmonic of a spherically focused beam (focused at 60 mm) and a modified Bessel beam transmitted from the 15 mm transducer. Figure 4 (a) shows about equal beamwidth at the focal point, and the second harmonic sidelobes of the modified Bessel beam has decreased about 6 dB compared to the first harmonic of a conventional Bessel beam. Outside the focal area, shown in figures (b) and (c), the beamwidth of the spherically focused beam increases, while the modified Bessel beam remains narrow for a large depth of field. The source pressure is here chosen lower than the maximum allowed value, giving an MI value of about 0.9, as this gives lower second harmonic sidelobes of the modified Bessel beam. Lu and Greenleaf [10] have used a similar approach where the central lobe was deleted. They were not concerned with harmonic imaging, but tried to avoid exceeding the safety limits in the near-field.

Corresponding results for a modified X wave are plotted in figure 5. The second harmonic of the modified X wave shows the same characteristics as the modified Bessel beam. Figure 6 shows the first and second harmonic X wave pulse where the y-axis is the lateral distribution and the x-axis is time (time has been converted to distance). The second harmonic in plot (b) shows less energy in the X-branches which is clearly seen to the right of the pulse center on the first harmonic in plot (a).

Figure 7 shows a comparison of the modified Bessel beam and the spherically focused beam in an attenuating medium like biological soft tissue. Attenuation is 0.3 dB/cm/MHz and the non-linearity parameter  $\beta = 4$ . Source pressure is chosen to

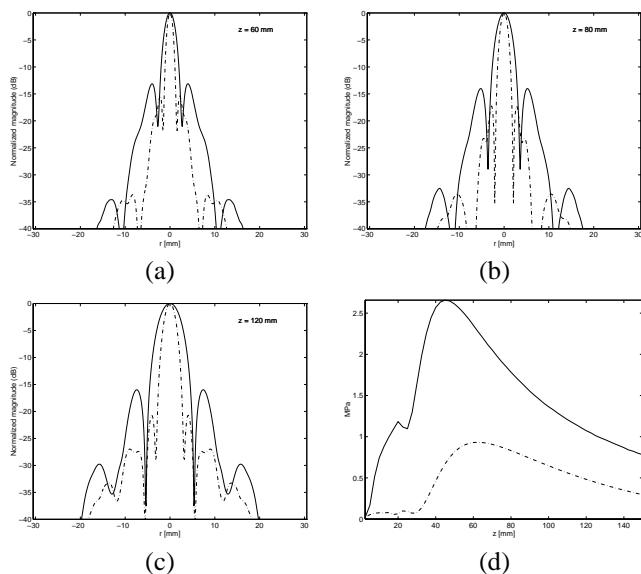


Fig. 5. First (solid line) and second (dotted line) of modified X wave (a), (b) and (c) Lateral field (dB) at  $z = 60, 80$  and  $120$  mm (d) Pulse peaks from  $z = 1 - 150$  mm

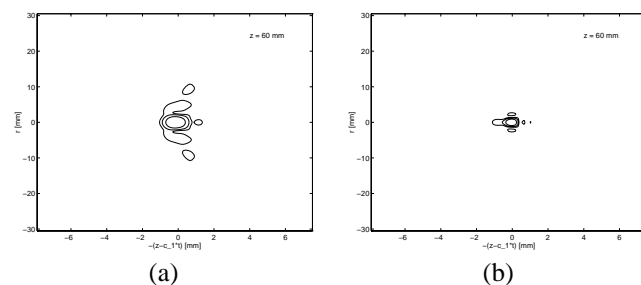


Fig. 6. -6, -12 and -18 dB contours of modified X wave pulse at  $z = 60$  mm (a) first harmonic (b) second harmonic.  $z - c_1 t$  is the distance away from the pulse center, located at  $z = c_1 t$ , where  $c_1$  is the propagation speed of the pulse peak.

give MI close to the safety limit. We see that the second harmonic sidelobes of the modified Bessel beam have grown due to higher initial pressure, but it has still improved second harmonic profile over the spherically focused beam outside the focal area.

As seen in figures 4, 5 and 7 (a)-(c) both the modified Bessel beam and X wave increase their lateral beamwidth as the beams propagate, and would hardly be termed limited diffraction beams since the focal properties vary with depth. Still, they have improved second harmonic properties, where the second harmonics are characterized by narrower beams with lower sidelobes and also have low near-field amplitude.

## V. CONCLUSION

Limited diffraction beams with a large aperture give a second harmonic beam with about half the beamwidth and almost unchanged sidelobes. Small apertures more often give reduced sidelobe levels in the second harmonic, but then the beamwidth is less improved. A modification of the beams where the central lobe was not transmitted, showed good second harmonic properties, characterized by narrow beams with decreased sidelobe level for large depth of field, and low relative near-field ampli-

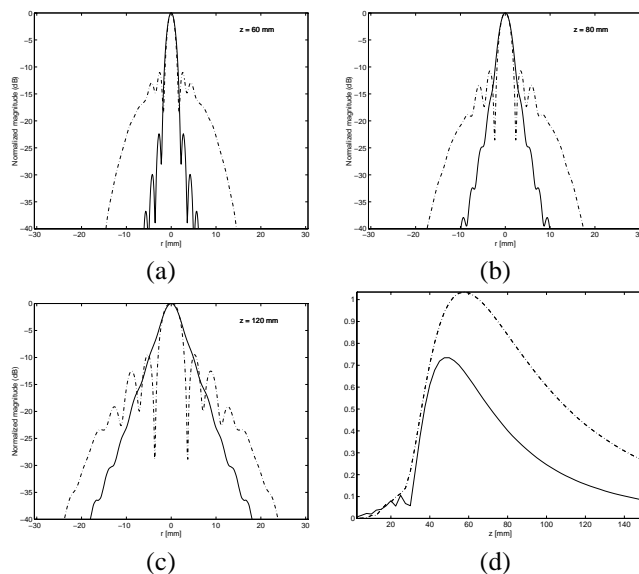


Fig. 7. Comparison of the second harmonic of a spherically focused (solid line) and modified Bessel beam (dotted line), with non-linearity parameter  $\beta = 4$ , and  $0.3$  dB/cm/MHz attenuation (a), (b) and (c) lateral field (dB) at  $z = 60, 80$  and  $120$  mm (d) axial amplitude from  $z = 1 - 150$  mm.

tude. A continuous wave modified Bessel beam was compared to continuous wave excitation of a spherically focused transducer, and showed improved lateral field outside the focal area even in an attenuating medium.

## ACKNOWLEDGMENT

We thank Professor Bjørn Angelsen, Norwegian University of Science and Technology, for stimulating discussions on nonlinear wave propagation, and the Department of Physics, University of Bergen for providing office space for one of the authors (J.-F.S.) for the completion of this paper.

## REFERENCES

- [1] J. Durmin, "Exact solutions for nondiffracting beams. I. The scalar theory," *J. Opt. Soc. Amer.*, vol. 4, pp. 651–654, Apr. 1987.
- [2] J.-Y. Lu and J. F. Greenleaf, "Nondiffracting X waves - exact solutions to free-space scalar wave equation and their finite aperture realizations," *IEEE Trans. Ultrason., Ferroelect., Freq. Contr.*, vol. 39, pp. 19–31, Jan. 1992.
- [3] J.-Y. Lu and J. F. Greenleaf, "Sidelobe reduction for limited diffraction pulse-echo systems," *IEEE Trans. Ultrason., Ferroelect., Freq. Contr.*, vol. 40, pp. 735–746, Nov. 1993.
- [4] P. T. Christopher and K. J. Parker, "New approaches to nonlinear diffractive field propagation," *J. Acoust. Soc. Amer.*, vol. 90, pp. 488–499, July 1991.
- [5] *Standard for Real-Time Display of Thermal and Mechanical Acoustic Output Indices on Diagnostic Ultrasound Equipment*. Amer. Inst. of Ultrasound in Medicine, Nat. Electr. Manufacturers Assoc., 1992.
- [6] M. A. Averkiou, D. N. Roundhill, and J. E. Powers, "A new imaging technique based on the nonlinear properties of tissues," *IEEE Ultrasonics Symp., Toronto*, Oct 1997.
- [7] S. Holm, "Bessel and conical beams and approximation with annular arrays," *IEEE Trans. Ultrason., Ferroelect., Freq. Contr.*, vol. 45, pp. 712–718, May 1998.
- [8] J.-Y. Lu and J. F. Greenleaf, "Ultrasonic nondiffracting transducer for medical imaging," *IEEE Trans. Ultrason., Ferroelect., Freq. Contr.*, vol. 37, pp. 438–447, Sept. 1990.
- [9] D. Ding and Z. Lu, "The second harmonic component in the Bessel beam," *Appl. Phys. Lett.*, vol. 68, no. 5, pp. 608–610, 1996.
- [10] J.-Y. Lu and J. F. Greenleaf, "Effect on  $J_0$  nondiffracting beam of deleting central elements of  $J_0$  annular array transducer," *Ultrason. Imaging* 13:203, 1991 (Abs.).